Exact Distributions for Stochastic Gene Expression Models with Bursting and Feedback

Niraj Kumar, Thierry Platini and Rahul V. Kulkarni

Original citation:
Kumar, N., Platini, T. and Kulkarni, R.V. (2014) Exact Distributions for Stochastic Gene Expression Models with Bursting and Feedback *Physical Review Letters* 113 (26) DOI 10.1103/PhysRevLett.113.268105

http://dx.doi.org/ 10.1103/PhysRevLett.113.268105

Publisher
American Physical Society

Exact Distributions for Stochastic Gene Expression Models with Bursting and Feedback

Niraj Kumar,[1,*] Thierry Platini,[2,†] and Rahul V. Kulkarni[1,‡]
[1]Department of Physics, University of Massachusetts Boston, Boston, Massachusetts 02125, USA
[2]Applied Mathematics Research Center, Coventry University, Coventry CV1 5FB, England
(Received 24 April 2014; published 31 December 2014)

Stochasticity in gene expression can give rise to fluctuations in protein levels and lead to phenotypic variation across a population of genetically identical cells. Recent experiments indicate that bursting and feedback mechanisms play important roles in controlling noise in gene expression and phenotypic variation. A quantitative understanding of the impact of these factors requires analysis of the corresponding stochastic models. However, for stochastic models of gene expression with feedback and bursting, exact analytical results for protein distributions have not been obtained so far. Here, we analyze a model of gene expression with bursting and feedback regulation and obtain exact results for the corresponding protein steady-state distribution. The results obtained provide new insights into the role of bursting and feedback in noise regulation and optimization. Furthermore, for a specific choice of parameters, the system studied maps on to a two-state biochemical switch driven by a bursty input noise source. The analytical results derived provide quantitative insights into diverse cellular processes involving noise in gene expression and biochemical switching.

DOI: 10.1103/PhysRevLett.113.268105 PACS numbers: 87.10.Mn, 02.50.-r, 82.39.Rt, 87.17.Aa

Introduction.—Cellular responses to environmental fluctuations often involve biochemical reactions that are intrinsically stochastic. For example, stochasticity (noise) plays an important role in processes leading to gene expression [1–3] and in biochemical switching between distinct states [4–7]. Regulation of noise in these processes is critical for the maintenance of cellular functions as well as for the generation of phenotypic variability among clonal cells. Quantitative modeling of mechanisms of noise regulation is a key step towards a fundamental understanding of cellular functions and variability.

Noise regulation in cells is typically implemented by regulatory proteins such as transcription factors (TFs). Recent research has demonstrated that, at the single-cell level, regulatory proteins are often produced in bursts [8–12]. Such proteins can be further involved in autoregulation (e.g., the Tat regulatory protein which controls the latency switch of HIV-1 viral infections) [13–19] or in downstream regulation of biochemical switches (e.g., switching of flagellar rotation states in bacterial chemotaxis) [4–7]. Some interesting questions arise from these observations: How does feedback from proteins produced in bursts regulate noise in gene expression and biochemical switching? How can gene expression parameters be tuned to optimize noise in the presence of bursting and feedback? The aim of this Letter is to address these questions by developing a gene expression model that combines bursting and feedback for which we obtain the exact stationary distribution.

Previous work on noise in gene expression has focused on exact analytical solutions for models with (a) bursting but no feedback effects [20] or (b) feedback effects but no protein production in bursts [18,19,21,22]. Similarly, previous work on noise-induced biochemical switching [7] does not consider the case of input noise source produced in bursts. In this Letter, we introduce a *single* model that addresses these gaps in the field. Our model reduces to multiple previously studied models in limiting cases. We obtain exact analytical distributions that significantly extend previously obtained results and lead to new insights.

Model.—A schematic representation of the model is shown in Fig. 1. Here, 0 and 1 represent the inactive and active states of the promoter, respectively. Note that the terms inactive or active are simply used to label the two states since protein production can occur from either state. Specifically, protein production from the inactive (active) state occurs with rate k_0 (k_1). Each production event results in a random burst of proteins, and we assume that these bursts are distributed geometrically with mean size b. The degradation rate of proteins is denoted by μ. The rate of

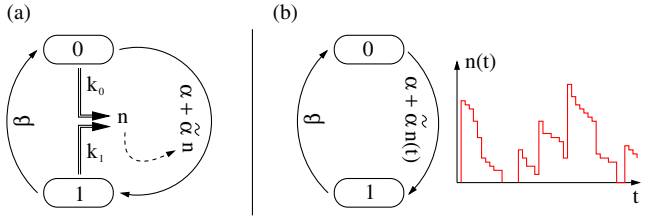

FIG. 1 (color online). (a) Schematic representation of the model. Protein bursts from inactive (active) state are generated with rate $k_0(k_1)$. Rate of transition from inactive to active state is $\alpha + \tilde{\alpha}n$, and that from active to inactive is β. (b) For $k_0 = k_1$ the model maps onto a two-state switch driven by a bursty input source.

switching from the active to inactive state is denoted by β. The rate at which the inactive state switches to the active state has two contributions: the spontaneous contribution with rate α, and the feedback contribution, with rate $\tilde{\alpha}n$ (where n is the number of proteins, and $\tilde{\alpha}$ measures the strength of the feedback). The linear dependence on n for the feedback term is consistent with experimental characterization of the genetic circuit for expression of HIV-1 Tat protein [13].

Since we allow protein production from both active and inactive states, the model can be used to analyze the effects of positive feedback as well as negative feedback. When $k_1 > k_0$, the feedback term enhances protein production leading to positive feedback. In contrast, $k_1 < k_0$ leads to negative feedback. For $k_1 = k_0$, protein production is independent of the promoter state. As indicated in Fig. 1(b), the model then corresponds to a bursty input noise source controlling switching between the two states. Thus, the same model can be used to analyze the impact of input protein noise on the statistics of a simple two-state switch [7].

Let $P_{\sigma,n}(t)$ denote the probability of finding, at time t, the promoter in state σ ($\sigma = 0, 1$) with n proteins in the cell. The temporal evolution of $P_{\sigma,n}(t)$ is given by the following master equations [23]:

$$\begin{aligned}\partial_t P_{0,n} &= k_0 \sum_{p=0}^{n} g(p) P_{0,n-p} + \mu(n+1)P_{0,n+1} \\ &\quad + \beta P_{1,n} - [k_0 + \alpha + \tilde{\alpha}n + \mu n]P_{0,n}, \\ \partial_t P_{1,n} &= k_1 \sum_{p=0}^{n} g(p) P_{1,n-p} + \mu(n+1)P_{1,n+1} \\ &\quad + (\alpha + \tilde{\alpha}n)P_{0,n} - [k_1 + \beta + \mu n]P_{1,n}, \end{aligned} \tag{1}$$

where $g(n) = b^n/(1+b)^{n+1}$ is the protein burst distribution. To proceed further, let us define the generating functions $G_\sigma(z,t) = \sum_n P_{\sigma,n}(t) z^n$ with $\sigma = 0, 1$. Correspondingly, Eq. (1) can be recast as

$$\begin{aligned}\partial_t G_0 &= k_0 \tilde{g} G_0 + \mu \partial_z G_0 + \beta G_1 \\ &\quad - (k_0 + \alpha) G_0 - (\tilde{\alpha} + \mu) z \partial_z G_0, \\ \partial_t G_1 &= k_1 \tilde{g} G_1 + \mu \partial_z G_1 + \alpha G_0 + \tilde{\alpha} z \partial_z G_0 \\ &\quad - (k_1 + \beta) G_1 - \mu z \partial_z G_1, \end{aligned} \tag{2}$$

where $\tilde{g}(z)$ is the generating function of the protein burst distribution given by $\tilde{g}(z) = 1/[1 + b(1-z)]$. In the long-time limit, Eq. (2) is used to derive an equation for the generating function of the protein steady-state distribution, $G(z) = G_0(z) + G_1(z)$. After a sequence of transformations (see Supplemental Material [24]), Eq. (2) reduces to a hypergeometric differential equation, leading to the solution

$$\begin{aligned} G(z) &= \left[\frac{1}{1 + b(1-z)}\right]^{k_1/\mu} \\ &\quad \times \frac{{}_2F_1[u, v | u + v + 1 - w | 1 - \phi\{1 + b(1-z)\}]}{{}_2F_1[u, v | u + v + 1 - w | 1 - \phi]}, \end{aligned} \tag{3}$$

where the quantities, u, v, w, and ϕ are related to model parameters by

$$\begin{aligned} u + v &= \frac{\Delta k + \alpha + \beta - \tilde{\alpha} k_1/\mu}{\mu + \tilde{\alpha}}, \qquad uv = \frac{\beta \Delta k}{\mu(\mu + \tilde{\alpha})}, \\ w &= \frac{\Delta k + \mu + \tilde{\alpha}(1+b)(1 - k_1/\mu)}{\mu + \tilde{\alpha}(1+b)}, \qquad \phi = \frac{\mu + \tilde{\alpha}}{\mu + \tilde{\alpha} + b\tilde{\alpha}}, \end{aligned} \tag{4}$$

with $\Delta k = k_0 - k_1$, and ${}_2F_1$ represents the Gaussian hypergeometric function. This solution for the generating function is the central result of this Letter. It can be shown that our result reduces to previously obtained results in different limiting cases (Supplemental Material [24]). It can be used to derive exact analytical results for several quantities of interest. For example, the steady-state probability that the promoter is in state 0 [$P_0 = G_0(1)$] is given by (see Supplemental Material [24])

$$\begin{aligned} P_0 &= \frac{\phi\beta}{\alpha + \beta + \frac{k_0 \tilde{\alpha} b}{\mu + \tilde{\alpha}(1+b)}} \\ &\quad \times \frac{{}_2F_1[u+1, v+1, u+v+2-w, 1-\phi]}{{}_2F_1[u, v, u+v+1-w, 1-\phi]}. \end{aligned} \tag{5}$$

Furthermore, Eq. (3) can be used to obtain an analytical expression for the protein steady-state distribution $P_n = P_{0,n} + P_{1,n}$ and to analyze the corresponding moments. These expressions lead to quantitative insights into multiple topics of current research interest as discussed below.

Regulation of protein noise.—There has been considerable focus in previous work on analyzing the effects of feedback on the noise $\eta = \langle n^2 \rangle / \langle n \rangle^2 - 1$ characterizing the protein steady-state distribution [13–16,25]. To analyze the impact of feedback, we first compare the noise for the case with feedback ($\tilde{\alpha} > 0$) to the case without feedback ($\tilde{\alpha} = 0$) in Figs. 2(a) and 2(b). It is interesting to observe that negative feedback increases the noise when compared to the case without feedback: $\eta(\tilde{\alpha})/\eta(0) > 1$. On the other hand, positive feedback leads to a decrease of noise $\eta(\tilde{\alpha})/\eta(0) < 1$. While this may appear surprising given previous results [26], this observation is consistent with recent results from simulations [16]. It should be further noted that negative feedback leads to a reduction in mean levels, whereas positive feedback increases mean levels; thus, the changes in η can be driven largely by changes in the mean levels. It follows that, to determine the effects of

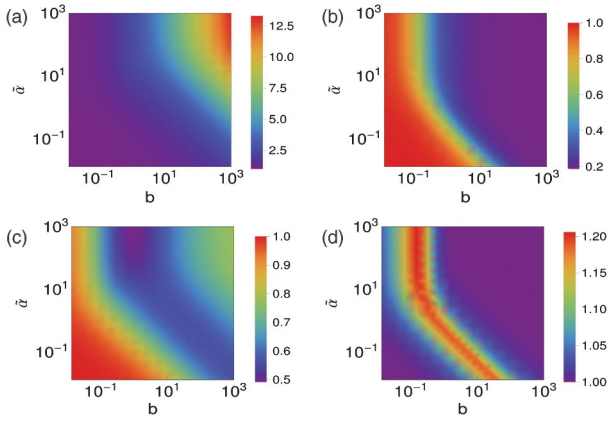

FIG. 2 (color). Protein noise regulation: In the upper panel, density plots for the noise ratio $\eta(\tilde{\alpha})/\eta(\tilde{\alpha}=0)$ as a function of b and $\tilde{\alpha}$ for (a) negative feedback ($k_0=10$, $k_1=0$) and (b) positive feedback ($k_0=0$, $k_1=10$). In the lower panel, comparison between the original and effective models: Density plots for $\eta/\eta_{\rm eff}$ are plotted as a function of b and $\tilde{\alpha}$ for (c) negative feedback ($k_0=10$, $k_1=0$) and (d) positive feedback ($k_0=0$, $k_1=10$). Other parameters are: $\alpha=\beta=\mu=1$.

feedback on noise, it is desirable to compare models which give rise to the same mean levels.

To address this issue, we introduce an effective model with no feedback that is characterized by a constant rate $\alpha_{\rm eff}$ for promoter switching from the inactive to the active state. The parameter $\alpha_{\rm eff}$ is determined analytically (Supplemental Material [24]) by the condition that the mean protein levels $\langle n\rangle$ and P_0 are identical in the original and effective models. The remaining parameters are the same as in the original model. In the following, we compare noise in protein distributions for the original and effective models.

Figures 2(c) and 2(d) illustrates the ratio $\eta/\eta_{\rm eff}$ for negative as well as positive feedback. For negative feedback, protein noise in the original model is lower than the noise in the effective model; i.e., the effect of negative feedback is to reduce noise. For positive feedback, as shown in Fig. 2(d), we observe that feedback increases the noise when compared to the noise for the effective model. Thus, in the context of regulation of protein noise, the results obtained indicate that the choice of reference model plays a critical role. In relation to the model without feedback, we observe that negative (positive) feedback increases (decreases) the noise. However, in relation to the effective model, which preserves the average number of proteins, the opposite behavior is observed.

Figures 2(c) and 2(d) also indicate that the effective model provides a useful approximation to the original model for a wide range of parameters, in particular, for positive feedback. In this case, for the range of parameters considered in Fig. 2(d), the effective model provides a good approximation in regions of parameter space for which a) $\alpha_{\rm eff}\approx\alpha$ or b) $\alpha_{\rm eff}\gg\beta$. In the former case, fluctuations in protein levels make a negligible contribution to the promoter switching rate, whereas the latter condition represents (almost) constitutive production of protein bursts, making the effective model indistinguishable from the original model. However, there is a class of problems for which the effective model is inadequate, and it is necessary to analyze the complete model. An important example includes noise optimization in the presence of feedback by varying system parameters, as discussed in the following.

Noise minimization.—Recent work [27] has analyzed noise minimization due to negative feedback for a model similar to the one outlined in Fig. 1. In this model, the binding of a TF switches its promoter to a repressed state, (i.e., set $k_1=0$) and the switching rate β corresponds to the dissociation rate of the TF from its promoter. In the limit $\beta\to\infty$, there is no feedback, since protein bursts are effectively produced constitutively with rate k_0. To examine noise minimization, the system parameters k_0 and β are varied subject to the constraint that the mean protein number $\langle n\rangle$ is held fixed. In particular, it is of interest to determine: (a) the minimum dissociation rate, $\beta_{\rm min}$, required for negative feedback to result in a reduction of noise relative to the model with no feedback and (b) the optimal rate β_c at which noise suppression is maximal. In the following, we explore the insights gained for this problem (for the model in Fig. 1) using exact analytical results for moments derived using Eq. (3).

Figure 3 illustrates the variation of protein noise η as a function of TF dissociation rate β, keeping the mean protein levels fixed by changing the transcriptional rate k_0. In the limit $\beta\to\infty$ (i.e., no feedback), we have $\eta=(1+b)/\langle n\rangle$. As β is reduced, the noise initially decreases, reaches a minimum value at $\beta=\beta_c$ and subsequently increases. In contrast, for the corresponding effective model with a constant rate of promoter transitions (as defined in the preceding paragraphs), we have $\eta>(1+b)/\langle n\rangle$ for all finite β; i.e., there is no noise reduction. This indicates that it is essential to consider the role of fluctuations in the rate

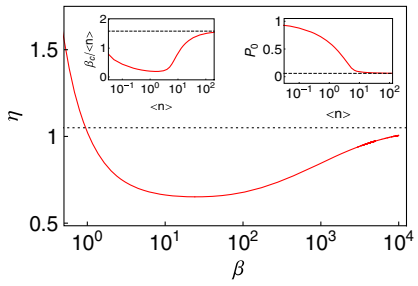

FIG. 3 (color online). Optimization of noise suppression in negative feedback: Noise is shown as a function of dissociation rate β for $\langle n\rangle=b=20$. Corresponding variations for the optimal dissociation rate β_c and the probability P_0 are plotted for different values of $\langle n\rangle$ in the inset, dotted lines representing the prediction of Ref. [27]. Other parameters are: $\mu=1$, $\alpha=0$, $\tilde{\alpha}=25$.

of promoter transitions (from the active to the repressed state) in understanding noise reduction due to negative feedback.

The parameter $\beta_{\min}$ can be determined by the condition that for $\beta = \beta_{\min}$, we have $\eta = (1+b)/\langle n\rangle$. The exact expression for η in combination with some approximations, specifically $P_0 = \beta/(\beta+\alpha+\tilde{\alpha}\langle n\rangle)$, can be used to derive the result obtained in [27] for $\beta_{\min}$ (Supplemental Material [24]). Our analysis indicates that this rate corresponds to $\beta_{\min} = P_0 k_0 b/(b+1)$ which implies that for noise reduction, the rate of TF dissociation must be greater than the rate of arrival of nonzero bursts of proteins.

Our results can also be used to analyze the optimal value $\beta = \beta_c$ at which noise suppression is maximal. The results derived in [27] using moment-closure approaches serve as a good approximation in the limit of large $\langle n\rangle$. Since our exact results apply for arbitrary parameter values, they can be used to connect large $\langle n\rangle$ results with those for low $\langle n\rangle$. As discussed below, this analysis leads to some interesting observations.

In Ref. [27], it was shown that the optimal value of dissociation rate β_c is linearly dependent on $\langle n\rangle$; i.e., $\beta_c/\langle n\rangle$ remains constant as $\langle n\rangle$ is varied by changing k_0. As expected, we recover this feature when $\langle n\rangle$ is large (see Fig. 3). However, for small $\langle n\rangle$ we see a strong deviation from the large $\langle n\rangle$ limit, characterized by nonmonotonic variation. Furthermore, this nontrivial variation in the optimal dissociation rate is also reflected in the probability of the promoter state being transcriptionally active, P_0. As shown in the figure, P_0 decreases monotonically with $\langle n\rangle$, and, in the limit of large $\langle n\rangle$, it approaches the result derived in Ref. [27]. Thus, our results predict that, for optimal noise suppression in low abundance TFs, the fraction of time that the promoter is active decreases as we increase TF concentration.

Switching statistics.—As noted in Fig. 1(b), when $k_0 = k_1$, the model analyzed can be mapped to a two-state system driven by a bursty input signal. Several cellular systems can be modeled (at a coarse-grained level) as two-state switches; thus, it is of interest to explore how such switches respond to fluctuating inputs [4–7]. The results obtained in this Letter lead to exact analytical expressions for the corresponding switch statistics.

The quantity of interest is the variance of the switch, $\sigma^2 = P_0(1-P_0)$, with P_0 given by Eq. (5). Note that Eq. (5) is valid for proteins produced in geometrically distributed bursts with mean burst size b. On the other hand, previous work [7] has considered the case such that each burst leads to creation of exactly one protein (i.e., protein dynamics is a simple birth-death process). Remarkably, there exists a mapping between the analytical solutions in these two cases (Supplemental Material [24]). Using this mapping, we obtain the following exact result for the problem considered in previous work [7]

$$P_0 = \frac{\beta(\mu+\tilde{\alpha})}{\tilde{\alpha}k + (\alpha+\beta)(\mu+\tilde{\alpha})} \times {}_1F_1\left[1, 1+\frac{\alpha+\beta}{\mu+\tilde{\alpha}}+\frac{\tilde{\alpha}k}{(\mu+\tilde{\alpha})^2}, -\frac{k}{\mu}\left(\frac{\tilde{\alpha}}{\mu+\tilde{\alpha}}\right)^2\right]. \quad (6)$$

As expected, the above expression, Eq. (6), reduces to analytical results derived in [7] (for $\alpha = 0$) in limiting cases. For example, in the slow switching limit, i.e., $\tilde{\alpha}k \ll \mu = 1$, Eq. (6) leads to $P_1 = 1 - P_0 = [\tilde{\alpha}/(1+\tilde{\alpha})]k/(\beta + [\tilde{\alpha}/(1+\tilde{\alpha})]k)$, which is identical to the result obtained in [7]. Similarly, in the fast switching limit $\tilde{\alpha}k \gg \mu = 1$, if we further set $\tilde{\alpha} \to \infty$ and $k \ll \mu = 1$, we obtain $P_1 = k(1+\beta)/(k+\beta)$, consistent with the result obtained in [7]. The exact result derived above, Eq. (6), allows for analysis of switching statistics beyond these limits, i.e., throughout parameter space.

Furthermore, the results derived can be used to explore how bursty protein production affects switching statistics. Figure 4(a) shows how the switch variance σ^2 depends on the burst size, b, and the average number of proteins, $\langle n\rangle$. Some interesting observations can be made which highlight the nontrivial variation of σ^2 with bursting. For large $\langle n\rangle$ values, σ^2 shows a nonmonotonic variation with b, with a maximum at a critical burst size, b_c [see Fig. 4(b)]. On the other hand, for low $\langle n\rangle$, we observe that σ^2 decreases monotonically with b with the maximum corresponding to $b_c \to 0$ [Fig. 4(b)]. These different behaviors can be understood based on the following observations: (1) For fixed $\langle n\rangle$, P_0 increases with increasing burst size b, and (2) for fixed b, P_0 decreases with increasing $\langle n\rangle$. Thus, in the limit $b \to 0$, for $\langle n\rangle$ such that $P_0 \geq 1/2$ we obtain a monotonic decrease in the variance $\sigma^2 = P_0(1-P_0)$ as b is increased. On the other hand, for $\langle n\rangle$ such that $P_0 < 1/2$ (in the limit $b \to 0$) we obtain a nonmonotonic variation with b.

Next, we focus on the variation of σ^2 with mean protein $\langle n\rangle$ for a fixed b. As can be seen in Fig. 4(a), it shows a

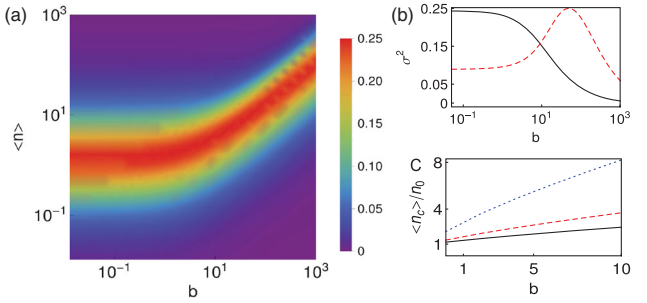

FIG. 4 (color). Two-state switch statistics. (a) Density plot for σ^2 is shown as a function of b and $\langle n\rangle$. (b) Variations of σ^2 with b for two different values of $\langle n\rangle$, 1 (solid line) and 10 (dashed line). In both (a) and (b), $\tilde{\alpha} = 1$. (c) Variation of $\langle n_c\rangle/n_0$ with b, different lines correspond to different values of feedback strength $\tilde{\alpha} = 0.5$ (solid line), 1 (dashed line), 3 (dotted line). In all plots, other parameters are: $\Delta k = \alpha = 0$, $\beta = \mu = 1$.

nonmonotonic variation, with σ^2 being maximum at a critical mean protein level, $\langle n_c \rangle$. Often, it is of interest to estimate the value $\langle n_c \rangle$ which maximizes the noise in switching statistics. In Fig. 4(c), we compare the mean-field estimate n_0 (obtained by replacing the fluctuating n by its mean value, $\langle n \rangle$) with the corresponding exact value. As indicated in the figure, deviation from the mean-field estimate is significant and increases with increasing burst size and feedback strength. Thus, the analytical results derived are useful in obtaining accurate estimates of parameters that maximize noise in switching statistics.

To conclude, we have studied an exactly solvable model that integrates key features of regulation of gene expression, specifically: bursting, promoter switching, and feedback, in a single model. The derived results provide new insights into the roles of bursting and feedback (both positive and negative) in fine-tuning noise in protein distributions. Furthermore, the results obtained can serve as building blocks for future studies focusing on noise optimization strategies by varying the underlying parameters. The model developed can also be applied to study the statistics of a simple two-state switch driven by a bursty protein noise source. Our results show that such bursty input noise can induce strong deviations in the optimal parameters for switch variance from the corresponding mean-field predictions. Thus, the development of analytical approaches, as outlined in this work, is an important ingredient for accurate quantitative modeling of stochastic cellular processes.

The authors acknowledge funding support from the NSF through Grants No. PHY-1307067 and No. DMS-1413111.

*niraj.kumar@umb.edu
†thierry.platini@coventry.ac.uk
‡rahul.kulkarni@umb.edu

[1] A. Raj and A. van Oudenaarden, Cell **135**, 216 (2008).
[2] A. Eldar and M. B. Elowitz, Nature (London) **467**, 167 (2010).
[3] A. Sanchez, S. Choubey, and J. Kondev, Annu. Rev. Biophys. **42**, 469 (2013).
[4] J. L. Spudich and D. E. Koshland, Nature (London) **262**, 467 (1976).
[5] H. C. Berg and E. M. Purcell, Biophys. J. **20**, 193 (1977).
[6] H. Park, P. Oikonomou, C. C. Guet, and P. Cluzel, Biophys. J. **101**, 2336 (2011).
[7] B. Hu, D. A. Kessler, W. J. Rappel, and H. Levine, Phys. Rev. Lett. **107**, 148101 (2011).
[8] L. Cai, N. Friedman, and X. S. Xie, Nature (London) **440**, 358 (2006).
[9] J. Yu, J. Xiao, X. Ren, K. Lao, and X. S. Xie, Science **311**, 1600 (2006).
[10] I. Golding, J. Paulsson, S. M. Zawilski, and E. C. Cox, Cell **123**, 1025 (2005).
[11] A. Raj, C. S. Peskin, D. Tranchina, D. Y. Vargas, and S. Tyagi, PLoS Biol. **4**, e309 (2006).
[12] J. Chubb, T. Trcek, S. Shenoy, and R. Singer, Curr. Biol. **16**, 1018 (2006).
[13] L. S. Weinberger, J. C. Burnett, J. E. Toettcher, A. P. Arkin, and D. V. Schaffer, Cell **122**, 169 (2005).
[14] T.-L. To and N. Maheshri, Science **327**, 1142 (2010).
[15] A. Singh and J. P. Hespanha, Biophys. J. **96**, 4013 (2009).
[16] M. Voliotis and C. G. Bowsher, Nucleic Acids Res. **40**, 7084 (2012).
[17] H. Feng, B. Han, and J. Wang, J. Phys. Chem. B **115**, 1254 (2011).
[18] J. E. M. Hornos, D. Schultz, G. C. P. Innocentini, J. Wang, A. M. Walczak, J. N. Onuchic, and P. G. Wolynes, Phys. Rev. E **72**, 051907 (2005).
[19] P. Visco, R. J. Allen, and M. R. Evans, Phys. Rev. Lett. **101**, 118104 (2008).
[20] V. Shahrezaei and P. S. Swain, Proc. Natl. Acad. Sci. U.S.A. **105**, 17256 (2008).
[21] R. Grima, D. R. Schmidt, and T. J. Newman, J. Chem. Phys. **137**, 035104 (2012).
[22] Y. Vandecan and R. Blossey, Phys. Rev. E **87**, 042705 (2013).
[23] N. G. van Kampen, *Stochastic Processes in Physics and Chemistry*, 3rd ed. (Elsevier, New York, 2007).
[24] See Supplemental Material at http://link.aps.org/supplemental/10.1103/PhysRevLett.113.268105 for detailed derivations.
[25] M. L. Simpson, C. D. Cox, and G. S. Sayler, Proc. Natl. Acad. Sci. U.S.A. **100**, 4551 (2003).
[26] A. Becskei and L. Serrano, Nature (London) **405**, 590 (2000).
[27] A. Gronlund, P. Lotstedt, and J. Elf, Nat. Commun. **4**, 1864 (2013).